An Improved Droop Control Method for DC Microgrids Based on Low Bandwidth Communication with DC Bus Voltage Restoration and Enhanced Current Sharing Accuracy

Lu, Xiaonan; Guerrero, Josep M.; Sun, Kai; Vasquez, Juan Carlos

Published in:
I E E E Transactions on Power Electronics

DOI (link to publication from Publisher):
10.1109/TPEL.2013.2266419

Publication date:
2014

Document Version
Early version, also known as pre-print

This paper is a preprint version of the final manuscript: X. Lu, J. M. Guerrero, K. Sun, J. C. Vasquez, "An improved droop control method for dc microgrids based on low bandwidth communication with dc bus voltage restoration and enhanced current sharing accuracy," *IEEE Trans. Power Electron.*, v. 99, no. PP, 2013.

An Improved Droop Control Method for DC Microgrids Based on Low Bandwidth Communication with DC Bus Voltage Restoration and Enhanced Current Sharing Accuracy

Xiaonan Lu, *Student Member, IEEE*, Josep M. Guerrero, *Senior Member, IEEE*, Kai Sun, *Member, IEEE*, Juan C. Vasquez, *Member, IEEE*

***Abstract*—Droop control is the basic control method for load current sharing in dc microgrid applications. The conventional dc droop control method is realized by linearly reducing the dc output voltage as the output current increases. This method has two limitations. First, with the consideration of line resistance in a droop-controlled dc microgrid, since the output voltage of each converter cannot be exactly the same, the output current sharing accuracy is degraded. Second, the DC bus voltage deviation increases with the load due to the droop action. In this paper, in order to improve the performance of the dc microgrid operation, a low bandwidth communication (LBC) based improved droop control method is proposed. In contrast with the conventional approach, the control system does not require a centralized secondary controller. Instead, it uses local controllers and the LBC network to exchange information between converter units. The droop controller is employed to achieve independent operation and average voltage and current controllers are used in each converter to simultaneously enhance the current sharing accuracy and restore the dc bus voltage. All of the controllers are realized locally, and the LBC system is only used for changing the values of the dc voltage and current. Hence, a decentralized control scheme is accomplished. The simulation test based on Matlab/Simulink and the experimental validation based on a 2×2.2 kW prototype were implemented to demonstrate the proposed approach.**

***Index Terms*—Current sharing accuracy, droop control, dc microgrid, low bandwidth communication, voltage deviation**

I. Introduction

In order to integrate different types of renewable energy sources and to electrify a remote area, the concept of the microgrid was proposed several years ago [1]. Recent literature on this topic is mostly focusing on ac microgrids, since the utility electrical grid relies on ac systems [2-6]. However, various sustainable energy sources and loads, such as photovoltaic (PV) modules, batteries, and LEDs, have natural dc couplings, so it is a more efficient method for connecting these sources and loads directly to form a dc microgrid by using dc-dc converters without ac-dc or dc-ac transformations. In a dc microgrid, there is no reactive power and there are no harmonics, so higher power quality and system efficiency are obtained compared to ac systems [7-15]. Therefore, there is an increasing focus on dc microgrids nowadays. The typical configuration of a dc microgrid is shown in Fig. 1 [7].

Since the renewable energy sources are decentralized connected to the common bus in a microgrid, the interfacing converters are connected in parallel. Power electronics interfacing converter control is a key issue in the operation of a microgrid, particularly for the load power sharing between different modules [16-19]. Various control methods have been proposed to achieve proper power sharing in a parallel converter system, such as master-slave control, circular-current-chain (3C) control, among others [20-21]. To satisfy the requirements of a distributed configuration, droop control without communication or with low bandwidth communication (LBC) is commonly accepted as an efficient power sharing method in a microgrid [22].

In a droop-controlled dc microgrid, the power sharing method is realized by linearly reducing the voltage reference as the output current increases [22]. Although droop control is widely employed as a decentralized method for load power sharing, its limitations should be noted. The output current sharing accuracy is lowered down because of the effect of the voltage drop across the line impedance. This effect is similar to the reactive power sharing of ac microgrids with inductive line impedances. To enhance the reactive power sharing accuracy in the ac microgrid with inductive line impedances, several methods have been proposed: the concept of virtual impedance was proposed to match the unequal line impedance [23]; a compensation method was proposed which used the remote voltage signal and employed an integrator term in the

Manuscript received January 16, 2013. This work was supported by the National Natural Science Foundation of China under Grant 51177083.

Xiaonan Lu is with the Department of Electrical Engineering, Tsinghua University, Beijing, 100084, China (e-mail: lxn04@mails.tsinghua.edu.cn).

Josep M. Guerrero is with the Institute of Energy Technology, Aalborg University, Aalborg, 9220, Denmark (e-mail: joz@et.aau.dk).

Kai Sun is with the Department of Electrical Engineering, Tsinghua University, Beijing, 100084, China (corresponding author, phone: +86-10-62796934, e-mail: sun-kai@mail.tsinghua.edu.cn).

Juan C. Vasquez is with the Institute of Energy Technology, Aalborg University, Aalborg, 9220, Denmark (e-mail: juq@et.aau.dk).

conventional *Q-V* droop control [24]; the voltage amplitude in *Q-V* droop control was replaced by $\dot{V}$ (*V* dot), which represents the time rate of the change of the voltage magnitude [25]; the voltage drop across the impedance was estimated in the grid-connected operation to reach the modified slope in the *Q-V* droop control [26].

In addition to the issue of current sharing accuracy in a dc microgrid, a voltage deviation is produced because droop control is realized by reducing the dc output voltage. To solve this problem, a centralized secondary controller was proposed to eliminate the voltage deviation; however, the influence of the line resistance was not taken into account [22]. At the same time, if there is a failure in the centralized controller, the function of voltage restoration cannot be achieved. A control scheme based on the average value of the dc output current in each of the converters has been presented [27]. This method was useful for restoring the dc bus voltage, while the effect of the enhancement of current sharing accuracy was not obvious enough. The reason for this is that only the average value of the dc output current was considered, while the dc output current was not individually controlled.

For the enhancement of power quality and the function of protection, the communication system in a microgrid cannot be completely removed. In order to meet the requirement of a distributed configuration, high frequency communication is not suitable enough for the practical microgrid. Power line communication (PLC) or LBC is commonly utilized [22, 28]. In this paper, an LBC-based, decentralized control method is proposed for dc microgrid applications. Particularly, the load power sharing is reached by using droop control. Meanwhile, a hybrid control scheme with additional average current and voltage controllers is employed in each converter module to simultaneously enhance the current sharing accuracy and restore the local bus voltage. The local controller of each converter individually adjusts each output current, so the current sharing accuracy is significantly improved. The LBC system is used only for the interchange of the dc voltage and current information, and all of the calculations and controllers are realized locally. Therefore, the control system is suitable for the distributed configuration in a microgrid and can provide higher reliability. The proposed control scheme has been tested for a range of communication delays. At the same time, the accurate proportional load current sharing can be achieved with different line resistances. The detailed model of the proposed control scheme is derived, and the stability of the system is analyzed. The simulation model based on Matlab/Simulink and the 2×2.2 kW prototype based on dSPACE 1103 were implemented to validate the proposed approach.

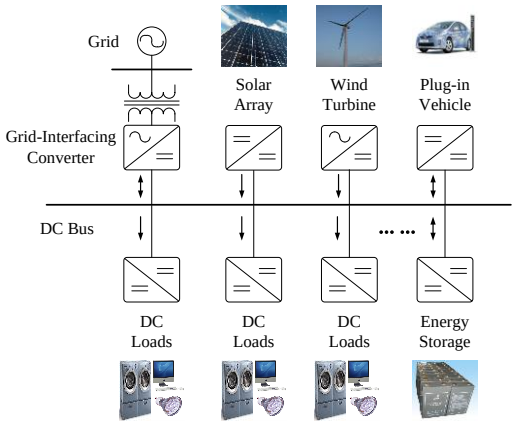

Fig. 1. Typical configuration of a dc microgrid.

The sections of this paper are organized as follows. Section II reviews the limitations of the conventional droop control method in dc microgrids. Section III introduces the principle of the proposed control scheme. Section IV analyzes the stability of the control system under different communication delays, line resistances and expected output current sharing proportion. Section V shows the simulation test of the control scheme by using Matlab/Simulink. Section VI demonstrates the approach by using a 2×2.2 kW prototype controlled by dSPACE 1103. Finally, Section VII summarizes the paper and gives the conclusions.

II. Limitations of The Conventional Droop Control Method in Dc Microgrids

The conventional droop control method in a dc microgrid is achieved by linearly reducing the voltage reference when the output current increases. The first limitation of the conventional droop control method is the degradation of the current sharing accuracy. Since the output voltage cannot be exactly the same due to the additional voltage drop across the line resistances, the load current sharing accuracy is lowered down. Second, the voltage deviation exists due to the droop action. The above two limitations of the conventional droop control method are analyzed in detail as follows.

A. Current Sharing Accuracy Degradation

The load current sharing in a dc microgrid is realized by an *I-V* droop controller. This controller can be implemented by means of a virtual resistance; this method is also named adaptive voltage positioning [29]. If the line resistance is taken into account, as in the reactive power sharing in ac microgrids with inductive line impedances, the dc output voltages for the local converters are not exactly the same. Hence, the current sharing accuracy is degraded. A detailed analysis of this problem is shown below.

A dc microgrid with two nodes is depicted in Fig. 2, where each converter is simplified by using the Thévenin equivalent model. The droop control method is expressed as

$$v_{\mathrm{dci}} = v_{\mathrm{dc}}^{*} - i_{\mathrm{dci}} \cdot R_{\mathrm{di}} \tag{1}$$

where v_{dci} is the output voltage of each converter, v_{dc}^{*} is the reference value of the dc output voltage, i_{dci} is the output current, R_{di} is the virtual resistance, and i = 1, 2.

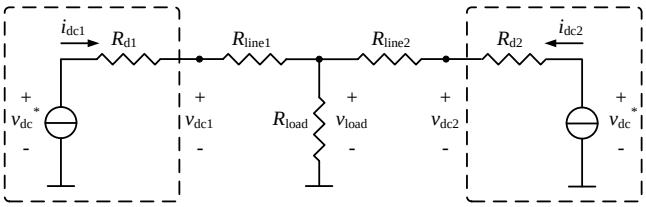

Fig. 2. Simplified model of a two-node dc microgrid.

Considering the relationship between dc voltage and current in (1), the value of the output resistance in the Thévenin equivalent model is equal to the virtual resistance, and the output voltage of the voltage source in the model is equal to v_{dc}^*, as shown in Fig. 2.

From Fig. 2, the following can be derived:

$$v_{load} = v_{dc}^* - i_{dc1} \cdot R_{d1} - i_{dc1} \cdot R_{line1} \tag{2a}$$

$$v_{load} = v_{dc}^* - i_{dc2} \cdot R_{d2} - i_{dc2} \cdot R_{line2} \tag{2b}$$

These expressions then yield the following:

$$\frac{i_{dc1}}{i_{dc2}} = \frac{R_{d2}}{R_{d1}} + \frac{R_{line2} - R_{d2} / R_{d1} \cdot R_{line1}}{R_{d1} + R_{line1}} \tag{3}$$

In the conventional droop-controlled dc microgrid, the dc output current of each converter is set to be inversely proportional to its virtual resistance. Hence, it is concluded from (3) that the current sharing error cannot be completely eliminated unless the following expression is satisfied:

$$\frac{R_{d1}}{R_{d2}} = \frac{R_{line1}}{R_{line2}} \tag{4}$$

Usually in a dc microgrid, it is assumed that the system is not so large that the line resistance only has a small value. Therefore, a larger virtual resistance R_{di} can be selected. Since $R_d >> R_{line1}$ and $R_d >> R_{line2}$, the following proceeds from (3):

$$\frac{i_{dc1}}{i_{dc2}} = \frac{R_{d2} + R_{line2}}{R_{d1} + R_{line1}} \approx \frac{R_{d2}}{R_{d1}} \tag{5}$$

However, the above assumption is only suitable for a small system. If the dc microgrid is larger, (5) cannot be satisfied. Meanwhile, with a large virtual resistance, the system stability is challenged. This is the first limitation of the conventional droop control method.

B. DC Voltage Deviation

As shown in (1), since droop control is employed, the dc voltage deviation can be found from the following formula:

$$\Delta v_{dci} = i_{dci} \cdot R_{di} \ (i=1, 2) \tag{6}$$

The analysis is also shown in Fig. 3. When the interfacing converter operates in the open-circuit condition, the dc voltage deviation is zero. When the dc output current is not equal to zero, the dc voltage deviation exists and its value varies with the load current. To guarantee that the voltage deviation does not exceed its maximum acceptable value, the value of the droop coefficient R_{di} should be limited:

$$R_{di} \le \frac{\Delta v_{dcmax}}{i_{dcfli}} \tag{7}$$

where i_{dcfli} is the full-load output current of converter #i.

The deviation of the output voltage is the second limitation of the conventional droop control method.

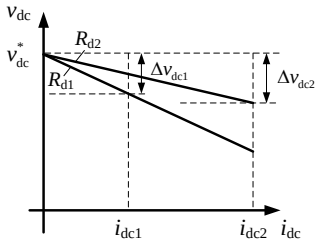

Fig. 3. Droop curve in a dc microgrid with different virtual resistances.

III. Principle of the Proposed Control Method

In order to solve the problems imposed by the two limitations of the conventional droop control method, an improved droop control method based on LBC is proposed. In this method, the enhancement of the current sharing accuracy and the restoration of local dc bus voltage are realized simultaneously. The LBC system is used for transferring the output voltages and currents of different converters. The detailed configuration of the proposed method is shown in Fig. 4. Here, the conventional droop control method is used to achieve proportional load current sharing approximately. Then, the output voltages and currents in the dc sides of the converters are transferred to the other converters using the LBC network. The average voltage and average current proportional-integral (PI) controllers are employed in each of the local control systems. For each average voltage controller, the reference value is v_{dc}^* and the average value of the dc voltage is controlled; as a result, each output voltage can be restored. At the same time, the reference value for each average current controller is i_{dc1}/k_1 or i_{dc2}/k_2, where k_1 and k_2 are the current sharing proportions, and the average value of i_{dc1}/k_1 and i_{dc2}/k_2 is the feedback variable. Therefore, the proportional output current sharing is guaranteed. All of the calculations and controllers are achieved locally. Thus, the proposed method is a type of decentralized method, which is suitable for the distributed configuration of a dc microgrid.

The comparison of the proposed method to the conventional current sharing method in parallel converter systems is shown in Table I. For the HBC-based method, like master-slave control, the control system is stable only when the HBC network is employed, otherwise the current references cannot be transferred among the converters. However, the proposed LBC-based method is an improved version of the conventional droop control. By using droop control, the current sharing is achieved by regulating the local output voltage, so that the communication is not necessary for guaranteeing the system stability. Communication here is only employed to reach auxiliary functionalities. The proposed LBC-based control method is used to solve the two main problems produced by droop control: current sharing accuracy degradation and voltage deviation. Hence, considering the dependency of communication, the viability of LBC-based methods in a microgrid is higher than that of HBC-based methods.

The advantage of the LBC-based method lays also in the reduced amount of data flowing in the communication network. Assuming that the sampling frequency is f_s, so the communication frequency of the HBC network is f_s. Meanwhile,

the communication frequency of the LBC network is selected to f_s/N. For an HBC-based control method, the data transferring is accomplished every control period, while for an LBC-based control method the data transferring is accomplished every N control periods. Hence, during the same length of time period, the amount of data on the communication network for the LBC-based method is highly reduced to 1/N in contrast with the HBC-based method. At the same time, when the scale of the microgrid is enlarged with the increasing number of interfacing converters, the data traffic for HBC network can be very busy. For instance, in the master-slave control, the current reference will be transferred to all of the slave converters. As a result, when the number of the converters increases, more data is required to flow through the communication network. If the LBC-based control strategy is employed, since the data transferring is performed every N control periods, the communication stress is highly reduced. Therefore, the LBC-based control method is more suitable than the HBC-based control method in a microgrid.

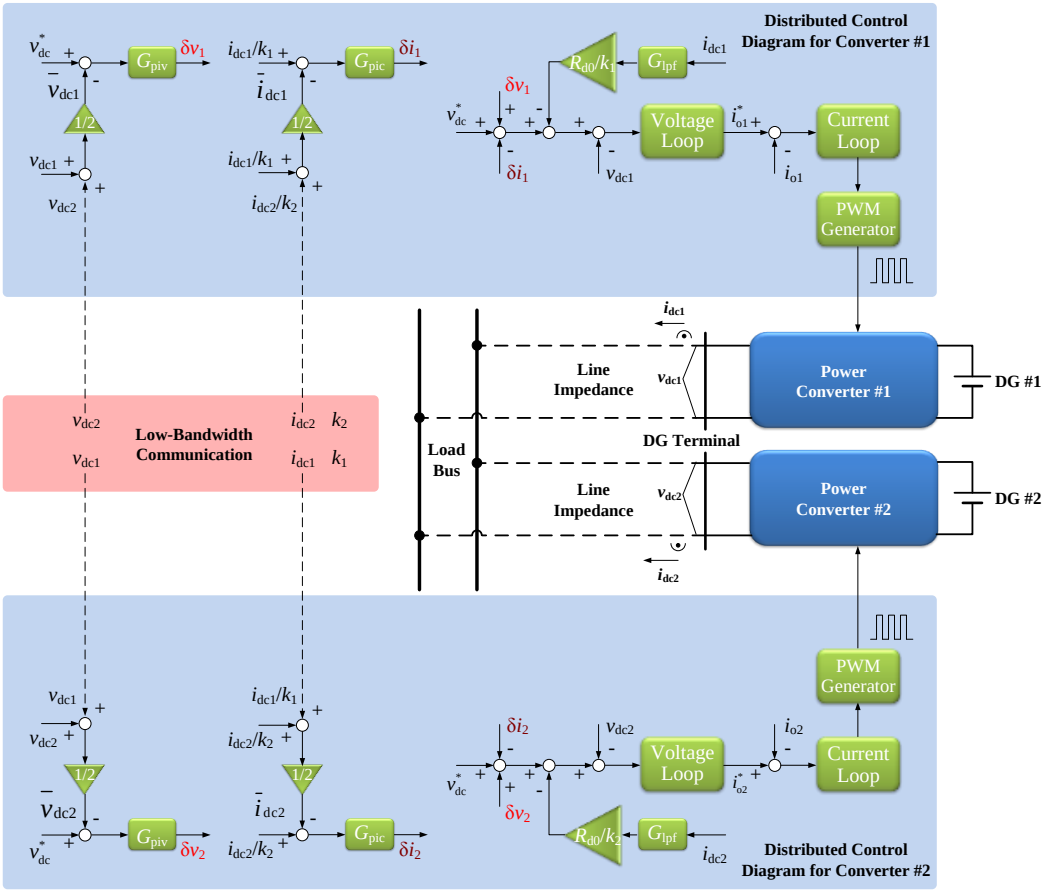

Fig. 4. Detailed configuration of the proposed control system.

TABLE I
COMPARISON OF DIFFERENT POWER SHARING METHODS

Power Sharing Method	Comm. Dependency	Viability	Sharing Accuracy	Voltage Quality
HBC[1]-based method [20-21]	High	Medium	High	High
Conventional droop control [22]	Low	High	Low	Low
LBC-based method	Low	High	High	High

It should be noticed that the dc input terminal is regarded as the voltage source in the proposed method and the ideal *I-V* droop curve is employed. In a real microgrid, the renewable energy source and the energy storage unit, such as the photovoltaic (PV) module and battery, have different droop characteristics, as shown in Fig. 5 (a) and (b). However, they can be combined to form an ideal dc voltage node which is the input of the interfacing converter, as shown in Fig. 5 (c). Especially in a dc residential microgrid, each house may have a PV and a battery. It is an efficient way to make the battery working in the voltage-controlled mode to form the local dc bus voltage and the other renewable energy sources are controlled to operate in the current feeding mode, which can inject or absorb power from the local dc bus. In this way, the sub-grid consisting of the PV and battery runs as a voltage node. Hence, the proposed method can be used to enhance the control performance of the interfacing converters between each dc voltage node and the dc bus.

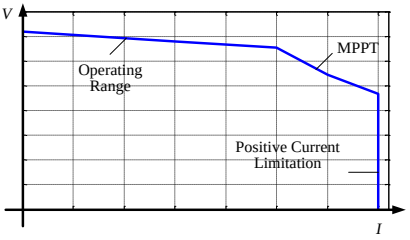

(a)

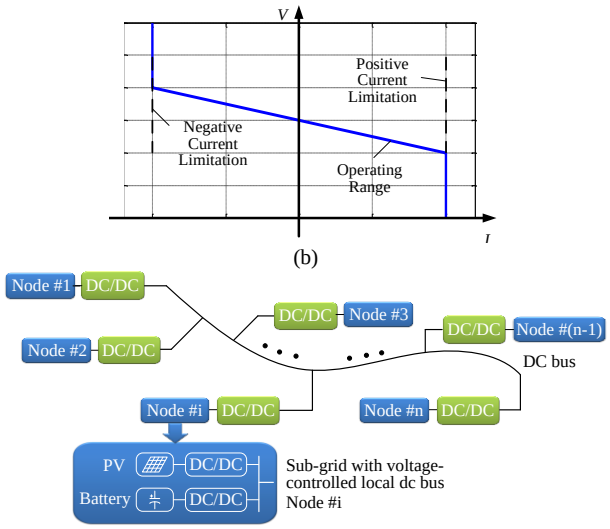

Fig. 5. Basic configuration of a dc microgrid with several voltage nodes. (a) Droop curve of PV modules. (b) Droop curve of batteries. (c) System configuration.

IV. Stability Analysis of The Proposed Control System

By analyzing the circuit in Fig. 2, the output currents can be expressed as

$$i_{dc1} = \alpha_1 \cdot v_{dc1} - \lambda \cdot v_{dc2} \tag{8}$$

$$i_{dc2} = \alpha_2 \cdot v_{dc2} - \lambda \cdot v_{dc1} \tag{9}$$

where

$$\alpha_1 = \frac{R_{line2} + R_{load}}{R_{line1}R_{line2} + R_{line2}R_{load} + R_{line1}R_{load}}$$

$$\alpha_2 = \frac{R_{line1} + R_{load}}{R_{line1}R_{line2} + R_{line2}R_{load} + R_{line1}R_{load}} \tag{10}$$

$$\lambda = \frac{R_{load}}{R_{line1}R_{line2} + R_{line2}R_{load} + R_{line1}R_{load}}$$

The detailed model of the control diagram for analyzing the system stability is shown in Fig. 6. The local voltage loop is expressed as

$$G_v = \frac{G_{pi}G_c}{1 + G_{pi}G_c} \tag{11}$$

where G_v, G_{pi} and G_c are the transfer functions of the voltage loop, local voltage PI controller and the local current controller. Here, G_c can be simplified as a delay unit.

To ensure the proportional sharing of the dc load current, the target of current sharing is set to

$$\frac{i_{dc1}}{i_{dc2}} = \frac{k_1}{k_2} \tag{12}$$

where k_1 and k_2 represent the proportion each converter shares.

From Fig. 6, the output voltage of each converter can be obtained as

$$v_{dc1} = [v_{dc}^* + (v_{dc}^* - \bar{v}_{dc1}) \cdot G_{piv} - (i_{dc1}/k_1 - \bar{i}_{dc1}) \cdot G_{pic} - R_{d0}/k_1 \cdot G_{lpf} i_{dc1}] \cdot G_v \tag{13}$$

$$v_{dc2} = [v_{dc}^* + (v_{dc}^* - \bar{v}_{dc2}) \cdot G_{piv} - (i_{dc2}/k_2 - \bar{i}_{dc2}) \cdot G_{pic} - R_{d0}/k_2 \cdot G_{lpf} i_{dc2}] \cdot G_v \tag{14}$$

where $\bar{v}_{dci}$ $(i = 1, 2)$ is the average value of the dc output voltage, and $\bar{i}_{dci}$ $(i = 1, 2)$ is the average value of the dc output current, which are shown as

$$\bar{v}_{dc1} = \frac{v_{dc1} + G_d \cdot v_{dc2}}{2} \tag{15}$$

$$\bar{i}_{dc1} = \frac{i_{dc1}/k_1 + G_d \cdot i_{dc2}/k_2}{2} \tag{16}$$

$$\bar{v}_{dc2} = \frac{G_d \cdot v_{dc1} + v_{dc2}}{2} \tag{17}$$

$$\bar{i}_{dc2} = \frac{G_d \cdot i_{dc1}/k_1 + i_{dc2}/k_2}{2} \tag{18}$$

For converter #1, v_{dc1} and i_{dc1} are the local variables, while v_{dc2} and i_{dc2} are transferred from converter #2 through the LBC network. Meanwhile, for converter #2, v_{dc2} and i_{dc2} are the local variables, while v_{dc1} and i_{dc1} are transferred from converter #1 through the LBC network. Hence, G_d is involved in (15) – (18) to model the communication delay, which can be expressed as the following:

$$G_d = \frac{1}{1 + \tau \cdot s} \tag{19}$$

where τ is the communication delay.

Meanwhile, in (13) and (14), G_{lpf} is the low-pass filter (LPF) for the output current in the droop control, which is expressed as

$$G_{lpf} = \frac{\omega_c}{s + \omega_c} \tag{20}$$

where ω_c is the cutting frequency of the LPF.

By combining (8) – (11) and (13) – (18), it yields

$$\frac{v_{dc1}}{v_{dc}^*} = [(1 - G_d)G_{piv} + \frac{(\alpha_2 k_1 + \lambda k_2)(1 + G_d)G_{pic}}{k_1 k_2} + 2(\frac{\alpha_2}{k_2} + \frac{\lambda}{k_1})R_{d0}G_{lpf} + \frac{2}{G_v}] \cdot \frac{2k_1^2 k_2^2 G_v^2 (1 + G_{piv})}{A_1 B_2 - A_2 B_1} \tag{21}$$

$$\frac{v_{dc2}}{v_{dc}^*} = [(1 - G_d)G_{piv} + \frac{(\alpha_1 k_2 + \lambda k_1)(1 + G_d)G_{pic}}{k_1 k_2} + 2(\frac{\alpha_1}{k_1} + \frac{\lambda}{k_2})R_{d0}G_{lpf} + \frac{2}{G_v}] \cdot \frac{2k_1^2 k_2^2 G_v^2 (1 + G_{piv})}{A_1 B_2 - A_2 B_1} \tag{22}$$

where

$$A_1 = k_1 k_2 G_v G_{piv} + (\alpha_1 k_2 + \lambda k_1 G_d)G_v G_{pic} + 2k_2 \alpha_1 R_{d0} G_v G_{lpf} + 2k_1 k_2$$

$$A_2 = k_1 k_2 G_v G_{piv} G_d - (\lambda k_1 + \alpha_1 k_2 G_d)G_v G_{pic} - 2k_1 \lambda R_{d0} G_v G_{lpf}$$

$$B_1 = k_1 k_2 G_v G_{piv} G_d - (\lambda k_2 + \alpha_2 k_1 G_d)G_v G_{pic} - 2k_2 \lambda R_{d0} G_v G_{lpf}$$

$$B_2 = k_1 k_2 G_v G_{piv} + (\alpha_2 k_1 + \lambda k_2 G_d)G_v G_{pic} + 2k_1 \alpha_2 R_{d0} G_v G_{lpf} + 2k_1 k_2$$

Taking the control diagram in converter #1 as an example, the stability of the closed-loop system can be tested by analyzing the location of the dominant closed-loop poles of (21) while varying the communication delays, the line resistances and the load current sharing proportions. The system parameters are listed in Table II.

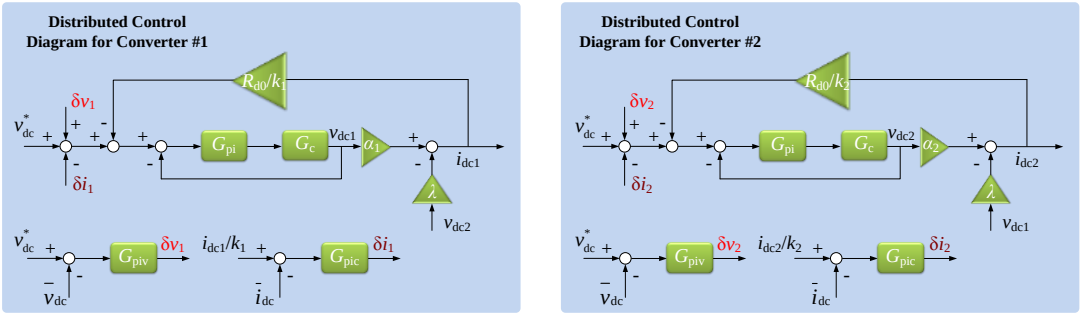

Fig. 6. Model of the control diagram for analyzing the system stability.

The closed-loop dominant poles of (21) for different communication delays are shown in Fig. 7. It should be noted that the communication delay affects six dominant poles of the closed-loop system. As the communication delay τ increases, these poles move toward the imaginary axis. Among different traces of these dominant poles, traces I, II, III, and IV terminate at the points P_1, P_2, P_3 and P_4, respectively. Traces V and VI are gradually extended to the imaginary axis, which challenge the system stability. However, although τ becomes as large as 0.3 s, the six dominant poles are located on the left half plane. Hence, the stability of the LBC-based control system can be guaranteed.

The closed-loop dominant poles for different line resistances are shown in Fig. 8. The value of R_{line1} is fixed, while the value of R_{line2} changes to test the stability of the control system for different conditions. The line resistance R_{line1} is set to 1 Ω and the value of R_{line2} is changed from 1/6 Ω to 6 Ω. Therefore, the conditions of $R_{line1} \geq R_{line2}$ and $R_{line1} < R_{line2}$ are taken into account. Fig. 8 shows that the value of the line resistance affects two dominant poles. As R_{line2} increases, there are two dominant poles move toward the imaginary axis, while the traces terminate at the points of P_1 and P_2. Therefore, the system stability can be ensured for different line resistances.

TABLE II
SYSTEM PARAMETERS

Item	Symbol	Value	Unit
Reference value of DC output voltage	v_{dc}^*	700	V
Line resistance (Converter #1 Side)	R_{line1}	1	Ω
Line resistance (Converter #2 Side)	R_{line2}	1/6 ~ 6	Ω
Load resistance	R_{load}	200	Ω
LPF cutting frequency	ω_c	126	rads^{-1}
Communication delay	τ	2 ~ 300	ms
Current sharing proportion (Converter #1)	k_1	1	-
Current sharing proportion (Converter #2)	k_2	1/2 ~ 2	-

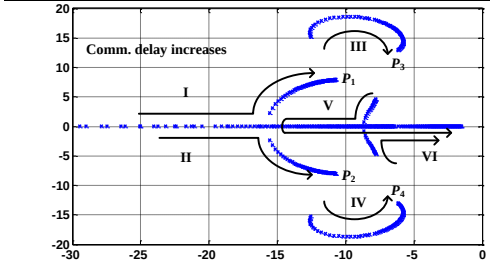

Fig. 7. Closed-loop dominant poles for different communication delays.

The effect of changing the load current sharing proportion over the closed-loop dominant poles is shown in Fig. 9. The relationship between i_{dc1} and i_{dc2} is shown in (12). To test the system stability, k_1 is fixed to 1 and k_2 varies from 1/2 to 2. Hence, the situations of either $i_{dc1} \geq i_{dc2}$ or $i_{dc1} < i_{dc2}$ are taken into account. The variation of k_2 affects two dominant poles of the system. Meanwhile, as k_2 increases, the two poles move away from the imaginary axis, so the control system remains stable.

As an important parameter of the control system, the communication delay should be properly selected according to the following criteria. First, considering the stability of the control system, all the closed-loop poles should be located on the left half plane of the s domain, as shown in Fig. 7. Second, considering the dynamics of the control system, the bandwidth of the control loop should be higher enough to achieve a proper dynamics. Since the communication delay acts on the outer dc voltage loop, considering the impact of the communication delay, the bandwidth of the dc voltage loop should be designed higher than its minimum acceptable value. For instance, if the sampling frequency is selected as 10 kHz, as the outer control loop, the bandwidth of the dc voltage loop is commonly set to be less than 100 Hz. Meanwhile, it should be higher than its minimum value; otherwise the dynamics of the voltage loop will be influenced. As shown in Fig. 10, it can be shown from (21) or (22) that the bandwidth of the voltage loop is reduced as the communication delay increases. Hence, the communication delay should be limited by the minimum value of the acceptable bandwidth, as depicted in the applicable region in Fig. 10.

It should be noted that the quantitative assessment of the control error is required to ensure the steady-state performance of the proposed control system. In Fig. 4, because an integrator is employed in the average voltage and average current controllers, the steady state error can be assumed to be negligible. At the same time, because each dc output current is individually controlled, proportional current sharing accuracy can be guaranteed. However, the output voltage of each converter cannot always be exactly the same as the reference value. From Fig. 2, the following can be derived:

$$v_{dc1} = R_{line1} \cdot i_{dc1} + v_{load} \tag{23}$$

$$v_{dc2} = R_{line2} \cdot i_{dc2} + v_{load} \tag{24}$$

Combining (23) – (24) and taking (12) into account yields:

$$\varepsilon_v = v_{dc1} - v_{dc2} = (R_{line1} - \frac{k_2}{k_1} R_{line2}) \cdot i_{dc1} \tag{25}$$

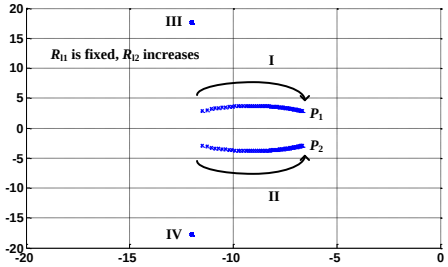

Fig. 8. Closed-loop dominant poles for different line resistances.

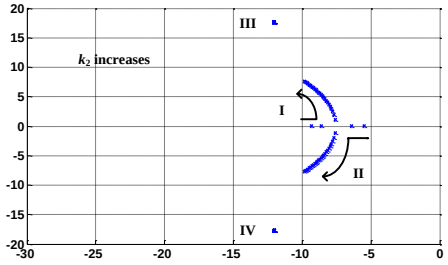

Fig. 9. Closed-loop dominant poles for different load sharing proportion.

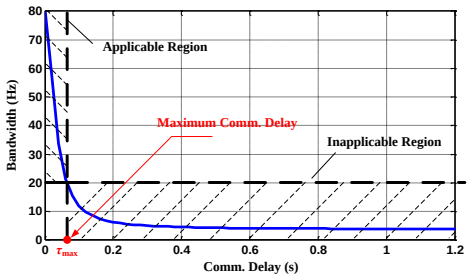

Fig. 10. Relationship between bandwidth of the outer voltage loop and communication delay.

From (25), it is concluded that the difference between each output voltage can be zero if and only if the following criterion is satisfied:

$$\frac{R_{\text{line1}}}{R_{\text{line2}}} = \frac{k_2}{k_1} \tag{26}$$

If the values of the line resistances and the current sharing proportion do not meet the relationship in (26), the dc output voltage in each converter cannot be the same. For this reason, only the average value of the dc output voltage is regulated to the reference value by using the PI controller. The dc output voltage and current cannot both be individually controlled due to the natural connection shown in Fig. 2 and the relationship in (25).

V. Simulation Test

Simulation test based on Matlab/Simulink is performed to demonstrate the feasibility of the proposed method. The system parameters are the same as those shown in Table II. Here, different line resistances are selected: R_{line1} is equal to 1 Ω, and R_{line2} is equal to 4 Ω. Meanwhile, the communication delay is set to 2 ms and the equal output current sharing is selected as the control objective.

Different resistive load are used to test the performance of the proposed control system. The responses for the voltage restoration and current sharing accuracy enhancement are shown in Fig. 11 and 12, where 200 Ω and 100 Ω load resistances are employed respectively. It is seen that when the proposed method is activated, the dc voltage of each converter is restored and the current sharing accuracy is enhanced. Meanwhile, the transient response with the step-up of the load current is shown in Fig. 13. It is also found that the proposed approach is still valid for the resistive load-step.

Meanwhile, different power load are used to test the performance of the proposed control system. The responses for the dc voltage and output power are shown in Fig. 14 and 15, where 2000 W and 4000 W power load are employed respectively. It is seen that when the proposed method is activated, the dc voltage of each converter is restored and the output power becomes equal. Meanwhile, the transient response with the step-up of the load power is shown in Fig. 16. It is also found that the proposed approach is still valid for the power load-step.

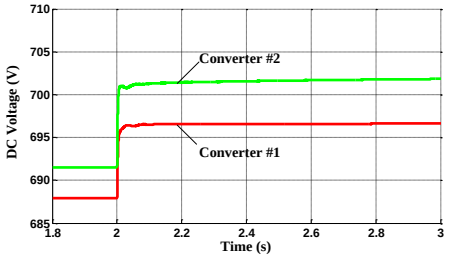

(a)

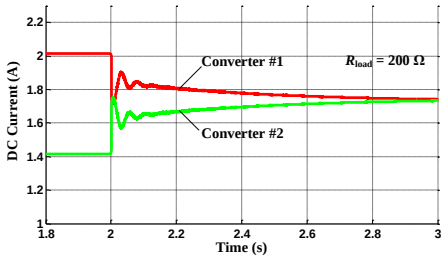

(b)

Fig. 11. The transient response when the LBC-based control method is activated (R_{load} = 200 Ω). (a) Voltage restoration. (b) Current sharing accuracy.

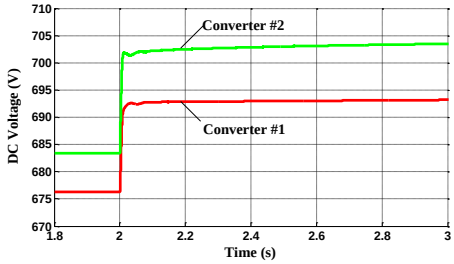

(a)

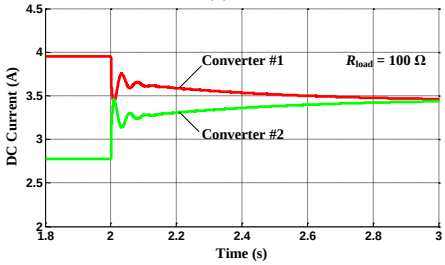

(b)

Fig. 12. The transient response when the LBC-based control method is activated (R_{load} = 100 Ω). (a) Voltage restoration. (b) Current sharing accuracy.

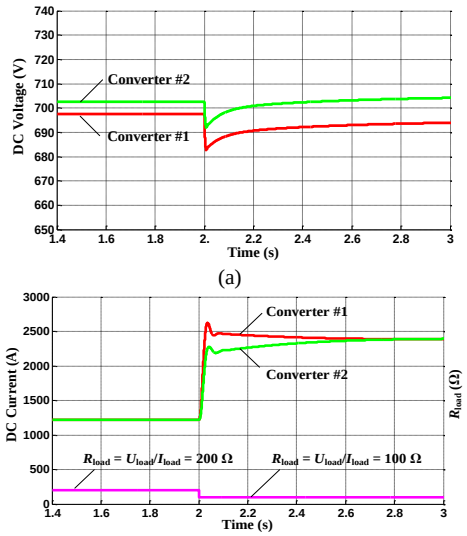

Fig. 13. The transient response with load step (R_{load} changes from 200 Ω to 100 Ω). (a) Voltage response. (b) Current response.

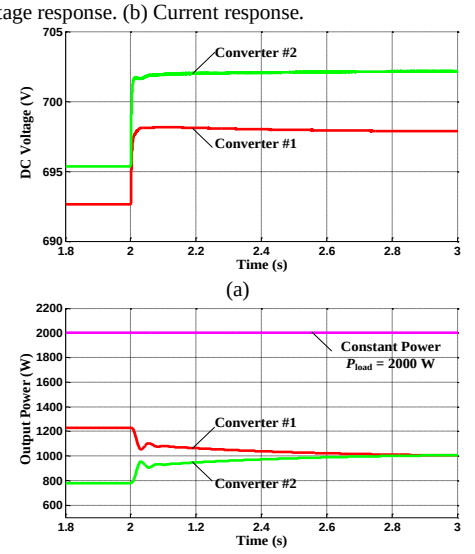

Fig. 14. The transient response when the LBC-based control method is activated (P_{load} = 2000 W). (a) Voltage restoration. (b) Power sharing accuracy.

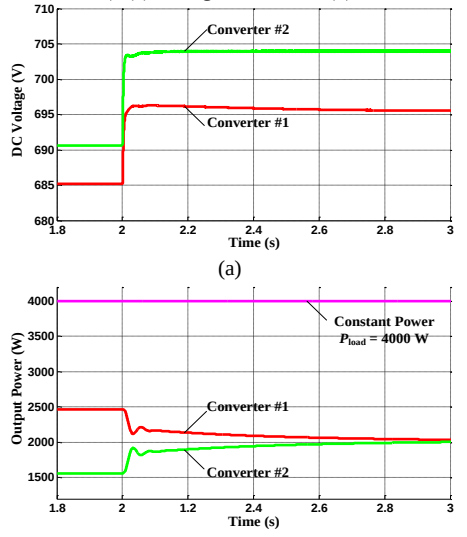

Fig. 15. The transient response when the LBC-based control method is activated (P_{load} = 4000 W). (a) Voltage restoration. (b) Power sharing accuracy.

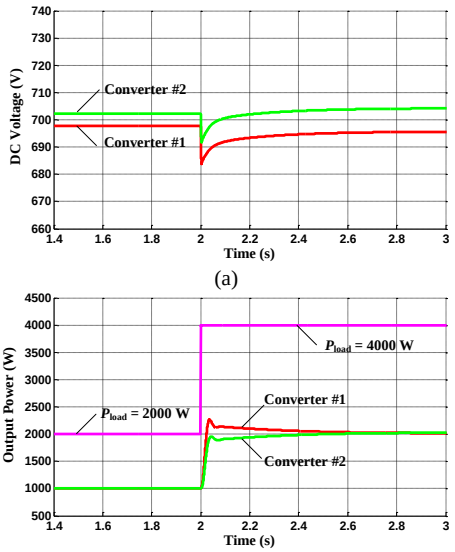

Fig. 16. The transient response with load step (P_{load} changes from 2000 W to 4000 W). (a) Voltage response. (b) Output power response.

VI. Experimental Validation

A 2×2.2 kW prototype with two parallel converters is implemented to validate the proposed control system. The system parameters are the same as those shown in Table II. The dc output voltage and current waveforms demonstrated the performance of the control system. With the proposed method, the dc voltage deviation involved in droop control can be eliminated and the dc output current sharing accuracy can be enhanced at the same time. Furthermore, the effects of different communication delays, line resistances and current sharing proportion are taken into account.

A. Voltage Restoration and Proportional Current Sharing Accuracy Enhancement

In the proposed control system, the functions of dc voltage restoration and current sharing accuracy enhancement can be achieved simultaneously. As shown in Fig. 17, before t = 0 s, the conventional droop control method is used. During this period, the dc voltage deviation is involved and the current sharing error is found in the dc output current waveform. To show the dc output current error, different line resistances are selected: R_{line1} is equal to 1 Ω, and R_{line2} is equal to 4 Ω. Meanwhile, equal load current sharing is selected as the control target ($k_1 = k_2$). At t = 0 s, the proposed control system is activated. With the proposed method, the average value of each output voltage is properly restored and the output currents become equal. It should be noted that the output voltages cannot all be equal; otherwise, the output current cannot be controlled, as demonstrated in (25). As it has been shown, this effect is due to the electrical network connection of the system, which is composed of different line resistances. However, although the output voltages are not exactly the same, each voltage level is within an acceptable range. Hence, the effectiveness of the control system is verified.

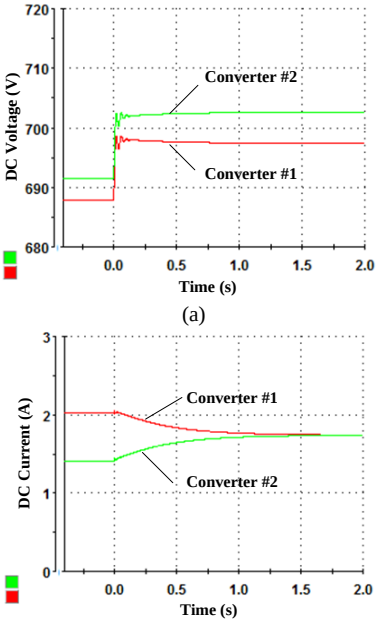

Fig. 17. The transient response when the LBC-based control method is activated. (a) Voltage restoration. (b) Current sharing accuracy.

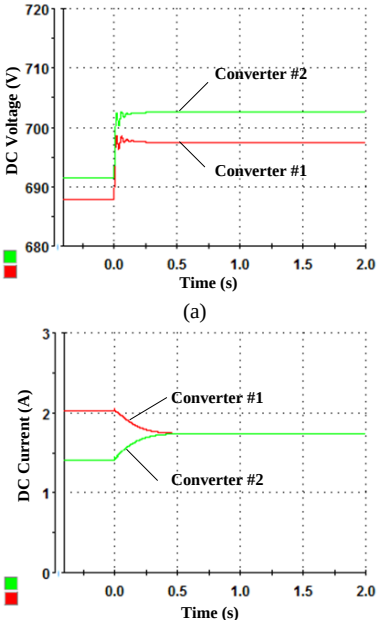

Fig. 18. The transient response when the LBC-based control method is activated (communication delay: 1 μs). (a) Voltage restoration. (b) Current sharing accuracy.

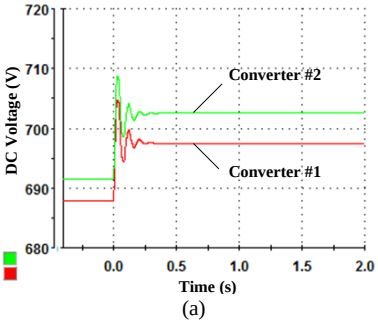

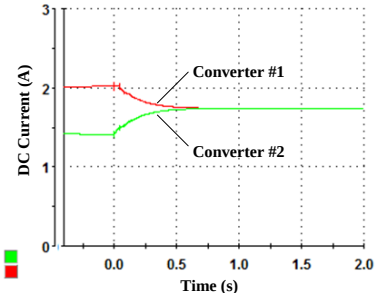

Fig. 19. The transient response when the LBC-based control method is activated (communication delay: 20 ms). (a) Voltage restoration. (b) Current sharing accuracy.

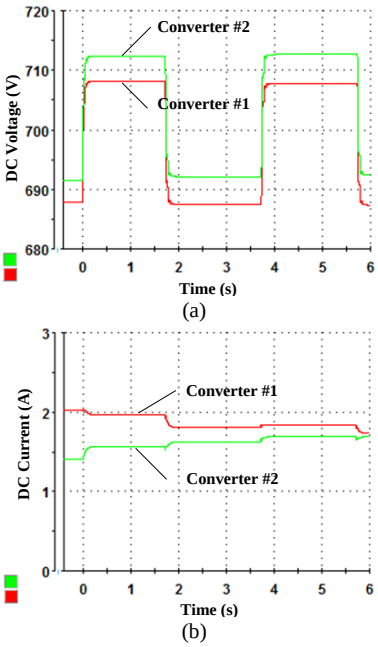

Fig. 20. The transient response when the LBC-based control method is activated (communication delay: 1 s). (a) Voltage restoration. (b) Current sharing accuracy.

B. Impact of Communication Delay

The proposed control system is implemented based on LBC, so that different communication delays are tested to study their impacts on the system performance. The communication delays include the following values: 1 μs, 20 ms and 1s. The corresponding dc output voltage and current waveforms are shown in Fig. 18 ~ Fig. 20. Here, R_{line1} is set to 1 Ω and R_{line2} is set to 4 Ω. The load current is equally shared ($k_1 = k_2$).

With a larger communication delay, the system becomes unstable. When the communication delay is set to 20 ms, the overshoot and oscillation of the dc output waveforms are more severe than when the communication delay is set to 1 μs; however, these waveform characteristics are still acceptable. When the communication delay is set to be as large as 1 s, the system becomes oscillatory. As shown in Fig. 20, the higher oscillation is found in the output voltage waveform. The reason for the oscillation is the large communication delay: the average value of the dc voltage is calculated with the present voltage value of the local converter and the delayed voltage value of the

other converter. Hence, it is concluded that with a higher communication delay, it is harder to keep the control system stable. However, although the delay is set to be as large as 20 ms (line period), the output performance is still acceptable. As a result, the viability of the LBC-based control diagram is validated.

C. Impact of Line Resistance

As shown in (5), the load current sharing is affected by the difference between the line resistances. To further test the applicability of the control system, different line resistances are tested. Here, R_{line1} is fixed to 1 Ω and R_{line2} is set to 4 Ω or 8 Ω. The corresponding output voltage and current waveforms are shown in Fig. 21 and Fig. 22. Here, equal current sharing is selected ($k_1 = k_2$). It can be seen that for different line resistances, the proposed control system is still providing the function of voltage restoration and current sharing accuracy enhancement as expected.

D. Impact of Current Sharing Proportion

To test the function of the enhancement of the dc load sharing, different current sharing proportion values are used. The transient responses of equal load current sharing are shown in Fig. 17, and the output voltage and current waveforms when $i_{dc1}/i_{dc2} = 0.5$ are shown in Fig. 23. Here, R_{line1} is equal to 1 Ω and R_{line2} is equal to 4 Ω. It can be seen that proportional load current sharing can be exactly realized by using the proposed method. The current sharing error before $t = 0$ s is shown in Fig. 23 (b). At $t = 0$ s, the proposed control system is activated. Then, the output current of each converter achieves the expected value. Hence, the load current sharing accuracy for different proportion values is validated.

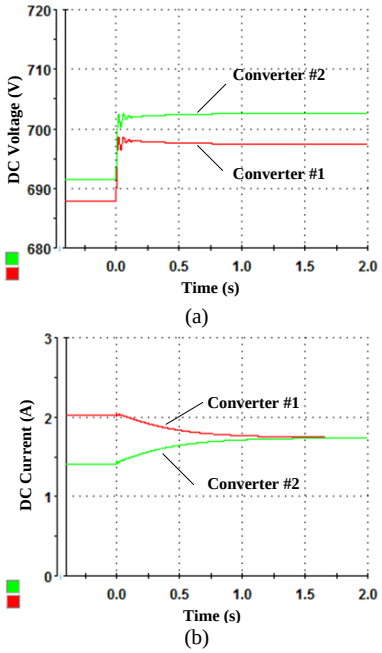

Fig. 21. The transient response when the LBC-based control method is activated (R_{line1} = 1 Ω, R_{line2} = 4 Ω). (a) Voltage restoration. (b) Current sharing accuracy.

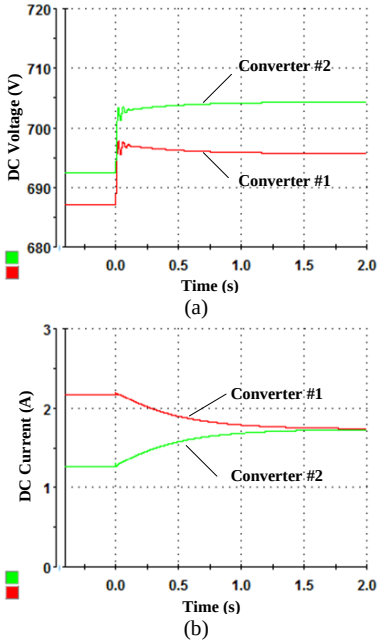

Fig. 22. The transient response when the LBC-based control method is activated (R_{line1} = 1 Ω, R_{line2} = 8 Ω). (a) Voltage restoration. (b) Current sharing accuracy.

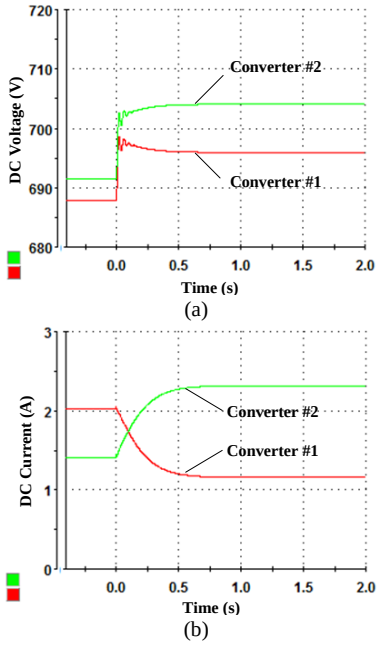

Fig. 23. The transient response when the LBC-based control method is activated (R_{line1} = 1 Ω, R_{line2} = 8 Ω). (a) Voltage restoration. (b) Current sharing accuracy.

VII. Conclusion

In this paper, an LBC-based distributed control method for a dc microgrid is proposed. Concretely, average voltage and average current PI controllers are employed to enhance the load current sharing accuracy and restore the local dc output voltage. The control loops are implemented locally, and the required voltage and current data are sent to the control system of the other converters through the LBC network. Hence, the distributed control system that meets the decentralized configuration of microgrid is realized. The model of the

proposed control system is obtained and the stability is analyzed. It is demonstrated that even though a high communication delay is employed (approximately 20 ms), the stability of the control system can also be guaranteed. At the same time, the viability of the proposed control system is ensured for different line resistances, and the proportional load current sharing is properly achieved. It is demonstrated that with the integral controller, the current sharing accuracy can be exactly reached. Meanwhile, the average value of the output voltage can be restored and each voltage is guaranteed to be within the acceptable range. The proposed approach is verified by simulation test based on Matlab/Simulink and experimental results from a 2×2.2 kW prototype.

REFERENCES

[1] R. Lasseter, A. Akhil, C. Marnay, J. Stevens, et al, "The certs microgrid concept - white paper on integration of distributed energy resources," *Technical Report*, U.S. Department of Energy, 2002.

[2] J. He and Y. W. Li, "An enhanced microgrid load demand sharing strategy," *IEEE Trans. Power Electron.*,vol. 27, no. 9, pp. 3984-3995, 2012.

[3] Y. W. Li and C. N. Kao, "An accurate power control strategy for power-electronics-interfaced distributed generation units operating in a low-voltage multibus microgrid," *IEEE Trans. Power Electron.*, vol. 24, no. 12, pp. 2977-2988, 2009.

[4] Q. C. Zhong, "Robust droop controller for accurate proportional load sharing among inverters operated in parallel," *IEEE Trans. Ind. Electron.*, vol. 60, no. 4, pp. 1281-1290, 2013.

[5] N. Pogaku, M. Prodanović and T. C. Green, "Modeling, analysis and testing of autonomous operation of an inverter-based microgrid," *IEEE Trans. Power Electron.*, vol. 22, no. 2, pp. 613-625, 2007.

[6] J. C. Vasquez, J. M. Guerrero, A. Luna, et al, "Adaptive droop control applied to voltage-source inverters operation in grid-connected and islanded modes," *IEEE Trans. Ind. Electron.*, vol. 56, no. 10, pp. 4088-4096, 2009.

[7] D. Dong, I. Cvetkovic, D. Boroyevich, W. Zhang, et al, "Grid-interface bi-directional converter for residential DC distribution systems – part one: high-density two-stage topology," *IEEE Trans. Power Electron.*, vol. 28, no. 4, pp. 1655-1666, 2013.

[8] L. Xu and D. Chen, "Control and operation of a DC microgrid with variable generation and energy storage," *IEEE Trans. Power Del.*, vol. 26, no. 4, pp. 2513-2522, 2011.

[9] K. Sun, L. Zhang, Y. Xing and J. M. Guerrero, "A distributed control strategy based on DC bus signaling for modular photovoltaic generation systems with battery energy storage," *IEEE Trans. Power Electron.*, vol. 26, no. 10, pp. 3032-3045, 2011.

[10] H. Kakigano, Y. Miura and T. Ise, "Low-voltage bipolar-type DC microgrid for super high quality distribution," *IEEE Trans. Power Electron.*, vol. 25, no. 12, pp. 3066-3075, 2010.

[11] X. She, A. Q. Huang, S. Lukic and M. E. Baran, "On integration of solid-state transformer with zonal DC microgrid," *IEEE Trans. Smart Grid*, vol. 3, no. 2, pp. 975-985, 2012.

[12] Y. –K. Chen, Y. –C. Wu, C. –C, Song and Y. –S. Chen, "Design and implementation of energy management system with fuzzy control for dc microgrid systems," *IEEE Trans. Power Electron.*, vol. 28, no. 4, pp. 1563-1570, 2013.

[13] S. R. Huddy and J. D. Skufca, "Amplitude death solutions for stabilization of dc microgrids with instantaneous constant-power loads," *IEEE Trans. Power Electron.*, vol. 28, no. 1, pp. 247-253, 2013.

[14] S. –M. Chen, T. –J. Liang and K. –R. Hu, "Design, analysis, and implementation of solar power optimizer for dc distribution system," *IEEE Trans. Power Electron.*, vol. 28, no. 4, pp. 1764-1772, 2013.

[15] H. Kakigano, Y. Miura and T. Ise, "Distribution voltage control for dc microgrids using fuzzy control and gain-scheduling technique," *IEEE Trans. Power Electron.*, vol. 28, no. 5, pp. 2246-2258, 2013.

[16] F. Blaabjerg, Z. Chen and S. B. Kjaer, "Power electronics as efficient interface in dispersed power generation systems," *IEEE Trans. Power Electron.*, vol. 19, no. 5, pp. 1184-1194, 2004.

[17] J. M. Carrasco, L. G. Franquelo, J. T. Bialasiewicz, et al, "Power-electronic systems for the grid integration of renewable energy sources: a survey," *IEEE Trans. Ind. Electron.*, vol. 53, no. 4, pp. 1002-1016, 2006.

[18] J. M. Guerrero, M. Chandorkar, T. L. Lee and P. C. Loh, "Advanced control architectures for intelligent microgrids – Part I: decentralized and hierarchical control," *IEEE Trans. Ind. Electron.*, vol. 60, no. 4, pp. 1254-1262, 2013.

[19] J. M. Guerrero, P. C. Loh, T. L. Lee and M. Chandorkar, "Advanced control architectures for intelligent microgrids – Part II: power quality, energy storage, and AC/DC microgrids," *IEEE Trans. Ind. Electron.*, vol. 60, no. 4, pp. 1263-1270, 2013.

[20] J. Rajagopalan, K. Xing, Y. Guo and F. C. Lee, "Modeling and dynamic analysis of paralleled dc/dc converters with master-slave current sharing control," *in Proc. IEEE APEC*, 1996, pp.678-684.

[21] T. F. Wu, Y. K. Chen and Y. H. Huang, "3C strategy for inverters in parallel operation achieving an equal current distribution," *IEEE Trans. Ind. Electron.*, vol.47, no.2, pp.273-281, 2000.

[22] J. M. Guerrero, J. C. Vasquez, J. Matas, L. G. Vicuña, et al, "Hierarchical control of droop-controlled AC and DC microgrids - a general approach toward standardization," *IEEE Trans. Ind. Electron.*, vol. 58, no. 1, pp. 158-172, 2011.

[23] J. M. Guerrero, L. G. de Vicuna, J. Matas, M. Castilla, et al, "Output impedance design of parallel-connected UPS inverters with wireless load-sharing control," *IEEE Trans. Ind. Electron.*, vol. 52, no. 4, pp. 1126–1135, 2005.

[24] C. K. Sao and P. W. Lehn, "Autonomous load sharing of voltage source converters," *IEEE Trans. Power Del.*, vol. 20, no. 2, pp. 1009–1016, 2005.

[25] C. T. Lee, C. C. Chu and P. T. Cheng, "A new droop control method for the autonomous operation of distributed energy resource interface converters," *IEEE Trans. Power Electron.*, vol. 28, no. 4, pp. 1980-1993, 2013.

[26] Y. W. Li and C. N. Kao, "An accurate power control strategy for power-electronics-interfaced distributed generation units operating in a low-voltage multibus microgrid," *IEEE Trans. Power Electron.*, vol. 24, no. 12, pp. 2977–2988, 2009.

[27] S. Anand, B. G. Fernandes and J. M. Guerrero, "Distributed control to ensure proportional load sharing and improve voltage regulation in low voltage DC microgrids," *IEEE Trans. Power Electron.*, vol. 28, no. 4, pp. 1900-1913, 2013.

[28] A. Pinomaa, J. Ahola and A. Kosonen, "Power-line communication-based network architecture for LVDC distribution system", *in Proc. IEEE Int. Symp. Power Line Commun. Appl.*, 2011, pp.358 -363.

[29] H. –H. Huang, C. –Y. Hsieh, J. –Y. Liao and K. –H. Chen, "Adaptive droop resistance technique for adaptive voltage positioning in boost DC–DC converters," *IEEE Trans. Power Electron.*, vol. 26, no. 7, pp. 1920-1932, 2011.

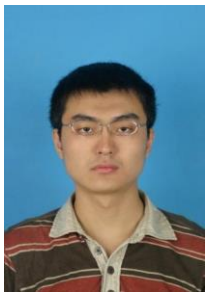

Xiaonan Lu (S'11) was born in Tianjin, China, 1985. He received the B.E. degree in electrical engineering from Tsinghua University, Beijing, China, in 2008. He is currently working towards his Ph.D. degree in Tsinghua University. From Sep. 2010 to Aug. 2011 he was a guest Ph.D. student at Department of Energy Technology, Aalborg University, Denmark.

His research interests include control of power electronics interfacing converters for renewable generation systems, multilevel converters, and matrix converters.

Mr. Lu is a student member of IEEE PELS Society.

Josep M. Guerrero (S'01-M'04-SM'08) received the B.S. degree in telecommunications engineering, the M.S. degree in electronics engineering, and the Ph.D. degree in power electronics from the Technical University of Catalonia, Barcelona, in 1997, 2000 and 2003, respectively. He was an Associate Professor with the Department of Automatic Control Systems and Computer Engineering, Technical University of Catalonia, teaching courses on digital signal processing, field-programmable gate arrays, microprocessors, and control of renewable energy. In 2004, he was responsible for the Renewable Energy Laboratory, Escola Industrial de Barcelona. Since 2011, he has been a Full Professor with the Department of Energy Technology, Aalborg University, Aalborg East, Denmark, where he is responsible for the microgrid research program. From 2012 he is also a guest Professor at the Chinese Academy of Science and the Nanjing University of Aeronautics and Astronautics. His research interests is oriented to different microgrid aspects, including power electronics, distributed energy-storage systems, hierarchical and cooperative control, energy management systems, and optimization of microgrids and islanded minigrids. Prof. Guerrero is an Associate Editor for the IEEE TRANSACTIONS ON POWER ELECTRONICS, the IEEE TRANSACTIONS ON INDUSTRIAL ELECTRONICS, and the IEEE Industrial Electronics Magazine. He has been Guest Editor of the IEEE TRANSACTIONS ON POWER ELECTRONICS Special Issues: Power Electronics for Wind Energy Conversion and Power Electronics for Microgrids, and the IEEE TRANSACTIONS ON INDUSTRIAL ELECTRONICS Special Sections: Uninterruptible Power Supplies systems, Renewable Energy Systems, Distributed Generation and Microgrids, and Industrial Applications and Implementation Issues of the Kalman Filter. He was the chair of the Renewable Energy Systems Technical Committee of the IEEE Industrial Electronics Society.

Kai Sun was born in Beijing, China, 1977. He received the B.E., M.E., and Ph.D. degrees in electrical engineering all from Tsinghua University, Beijing, China, in 2000, 2002, and 2006, respectively. In 2006, he joined the faculty of Tsinghua University as a Lecturer of Electrical Engineering, where he is currently an Associate Professor. From Sep. 2009 to Aug. 2010 he was a Visiting Scholar at Department of Energy Technology, Aalborg University, Denmark.

He has authored more than 50 technical papers, including 5 international journal papers. His main research interests are power converters for renewable generation systems, AC motor drives and AC-AC converters.

Juan C. Vasquez (M'12) received the B.S. degree in Electronics Engineering from Autonoma University of Manizales, Colombia in 2004 where he has been teaching courses on digital circuits, servo systems and flexible manufacturing systems. In 2009, He received his Ph.D. degree from the Technical University of Catalonia, Barcelona, Spain in 2009 at the Department of Automatic Control Systems and Computer Engineering, from Technical University of Catalonia, Barcelona (Spain), where he worked as Post-doc Assistant and also teaching courses based on renewable energy systems. Currently, he is an Assistant Professor at Aalborg University in Denmark. His research interests include modeling, simulation, networked control systems and optimization for power management systems applied to Distributed Generation in AC/DC Microgrids.